Drug Design, Development and Therapy

Dovepress

open access to scientific and medical research

Open Access Full Text Article

ORIGINAL RESEARCH

Mucoadhesive Nanoparticles Enhance the Therapeutic Effect of Dexamethasone on Experimental Ulcerative Colitis by the Local Administration as an Enema

Kai Dong[1,2], Shu-Jing Deng[2], Bin-Yang He[2], Zi-Yang Guo[2], Ze-Lin Guan[2], Xue Leng[2], Rui-Rui Ma[2], Dan-Yang Wang[2], Jian-Feng Xing[2], Cui-Yu You[1]

[1]Department of Pharmacy, The First Affiliated Hospital of Xi'an Jiaotong University, Xi'an, Shaanxi, People's Republic of China; [2]School of Pharmacy, Xi'an Jiaotong University, Xi'an, Shaanxi, People's Republic of China

Correspondence: Jian-Feng Xing, School of Pharmacy, Xi'an Jiaotong University, 76 Yanta West Road, Xi'an, 710061, Shaanxi, People's Republic of China, Tel +86-29-82655139, Fax +86-29-82655139, Email xajdxjf@mail.xjtu.edu.cn; Cui-Yu You, Department of Pharmacy, The First Affiliated Hospital of Xi'an Jiaotong University, Xi'an, Shaanxi, People's Republic of China, Tel +86-29-85323241, Fax +86-29-85323240, Email ycy720123@163.com

Background: As the first-line drug to treat ulcerative colitis (UC), long-term use of glucocorticoids (GCs) produces severe toxic and side effects. Local administration as enema can increase the local GCs concentrations and reduce systemic exposure to high oral doses by directly delivering GCs to the inflammation site in the distal colorectum. However, UC patients are often accompanied by diarrhea, leading to the short colonic residence time of GCs and failure to exert their function fully.

Purpose: A kind of mucoadhesive nanoparticles (NPs) loading different dexamethasone derivatives (DDs) were developed, which could attach to the positively charged inflammatory colonic mucosa through electrostatic adsorption after administered by enema, thereby improving the local concentration and achieving effective targeted therapy for UC.

Methods: Two DDs, dexamethasone hemisuccinate and dexamethasone phosphate, were synthesized. In NPs preparation, The core PEI-DDs NPs were built by the electrostatic adsorption of DDs and the cationic polymer polyethyleneimine (PEI). Then, the natural polyanionic polysaccharide sodium alginate (SA) was electronically coated around NPs to construct the final SA-PEI-DDs NPs, followed by the in vitro stability and release tests, in vitro and in vivo colonic mucosal adhesion tests. In the in vivo anti-UC test, the experimental colitis mice were induced by 2,4,6-trinitrobenzenesulfonic acid. The body weight and disease activity index changes were measured, and the myeloperoxidase activity, pro-inflammatory cytokines concentration, and hematoxylin and eosin staining were also investigated to evaluate the therapeutic effect of NPs.

Results: The structures of two DDs were demonstrated by ^{1}H-NMR and MS. Both NPs were negatively charged and achieved high loading efficiency of DDs, while their particle sizes were significantly different. NPs showed good stability and sustained release properties in the simulated colonic environment. Moreover, the negative charge on the of NPs surface made them easier to adhere to the positively charged inflammatory colonic mucosa, thereby enhancing the enrichment and retention of DDS in the colitis site. Furthermore, the NPs exhibited better therapeutic effects than free Dex on the experimental colitis mice induced by TNBS through the enema rectal.

Conclusion: These results indicated the mucoadhesive NPs as a kind of novel nano-enema showed great potential to achieve efficient treatment on UC.

Keywords: ulcerative colitis, glucocorticoids, mucoadhesive, polyethyleneimine, sodium alginate

Introduction

Ulcerative colitis (UC) is a chronic inflammatory bowel disease characterized by diffuse mucosal inflammation in the distal colon and rectum.[1,2] UC has a long course of the disease and is prone to recurrence, thus seriously affecting patients' life quality. Glucocorticoids (GCs) are the first-line drugs for patients with moderate to severe UC, which can

Received: 17 September 2022
Accepted: 9 January 2023
Published: 24 January 2023

inhibit the production of inflammatory mediators (such as leukotrienes, prostaglandins, etc.), cytokines [such as interleukins, tumor necrosis factor-α (TNF-α), interferon, etc.] and nitric oxide (NO) by regulating gene transcription.[3–6] However, since GCs affect substance metabolism, long-term oral administration of GCs induces severe systemic side effects, including endocrine disorders, cardiovascular diseases, osteoporosis, ophthalmic diseases, nervous system diseases, gastrointestinal adverse reactions, etc.[7,8] Therefore, targeted delivery of GCs to the colitis site improves the local anti-inflammatory effect of GCs and reduces their systemic side effects.

Enema administration is commonly used to treat intestinal diseases.[9–11] Research reports that two-thirds of UC patients with diffuse inflammation will occur in the distal colon, which needs local enema administration. Therefore, enema administration is more conducive to exerting the effect of drugs than oral administration.[12,13] The enema formulations can deliver medications directly to the site of inflammation in the distal colorectum, thereby providing increased local tissue drug concentrations without systemic exposure to large doses taken orally.[14,15] However, patients with UC are often accompanied by diarrhea, leading to the short residence time of drugs in the colon and the inability to exert their therapeutic effects fully.[16,17] Nano drug delivery system (NDDS) is an effective means to solve the above problems. The loss of epithelial barrier function in inflamed colonic tissues of UC patients leads to increased mucosal permeability, which allows the NDDS to passively target the inflamed colonic tissue through an epithelial-enhanced permeability and retention (eEPR) effect.[18,19] Besides, the colon physiological characteristics of UC patients are changed due to the intestinal inflammation, manifested by the depletion of colonic mucosal mucus and the large amounts of positively charged proteins accumulation in the inflammatory tissue, such as antimicrobial peptides, bactericidal/permeability-increasing proteins.[20–22] Therefore, the damaged colonic epithelial surface accumulates large amounts of positive charges, significantly different from the negatively charged normal colonic mucosa. The NDDS with negative charges on the surface can adhere to the inflammatory mucosa with the help of electrostatic adsorption force to reduce the drug loss caused by diarrhea in UC patients. Hence, NDDS with specific charges shows good potential application prospects for site-specific treatment of UC.

The treatment of UC by enema administration needs to maintain a high local GCs concentration, which requires the drug carrier with high drug-loading efficiency.[23] However, it is difficult for most nano-drug delivery systems to achieve high loading on GCs due to their hydrophobicity.[24] Preparing the water-soluble GCs derivatives by chemical modification, combined with the oppositely charged polymers to construct nanoparticles, can achieve high GCs loading.[25] This study used a typical GC, dexamethasone (Dex), as a model drug to synthesize Dex derivatives (DDs) containing different anionic functional groups by the esterification method. Then, the DDs and the hydrophilic cationic polymer polyethyleneimine (PEI) were self-assembled to construct the positively charged PEI-DDs nanoparticles (NPs). PEI is a cation-rich polymer commonly used to deliver negatively charged nucleic acid and protein drugs.[26,27] PEI has also been used as an immune adjuvant and chelating agent for water purification.[28,29] It has been reported that the cation-rich PEI can bind to negatively charged lipopolysaccharide (LPS) and inhibit the expression of TNF-α in macrophages caused by LPS, ultimately suppressing the inflammatory response.[30] PEI contains a variety of amino groups (primary amine, secondary amine, and tertiary amine), which results in electrostatic, hydrogen bond, and hydrophobic interaction between PEI and DDs. Therefore, the PEI and DDs can self-assemble to form NPs through these multiple noncovalent forces and realize the efficient loading of DDs.

Sodium alginate (SA) is a polysaccharide carbohydrate sodium salt extracted from Kelp or Sargasso. It is also a widely used natural polymer material for medicine due to its low toxicity, good biocompatibility, and degradability.[31,32] The excellent mucosal adhesion of SA makes it attach to the mucosa through the interaction between the molecular chain and mucin and increase the viscosity of mucus.[33] In this study, to realize the adhesion to the positively charged inflammatory colonic mucosa, the PEI-DDs NPs were further self-assembled with SA to build the final bilayer complex NPs, SA-PEI-DDs (Scheme 1). The SA-PEI-DDs NPs can be administered directly to the inflammatory site of the distal colorectum through enema administration. The DDs can be efficiently targeted to the affected area through the electrostatic interaction between SA and the inflammatory mucosa, which improves the therapeutic effect by increasing the drug concentration in the inflammatory site and effectively reduces the DDs' systemic toxicity. This study provides a novel idea for applying GC in UC treatment.

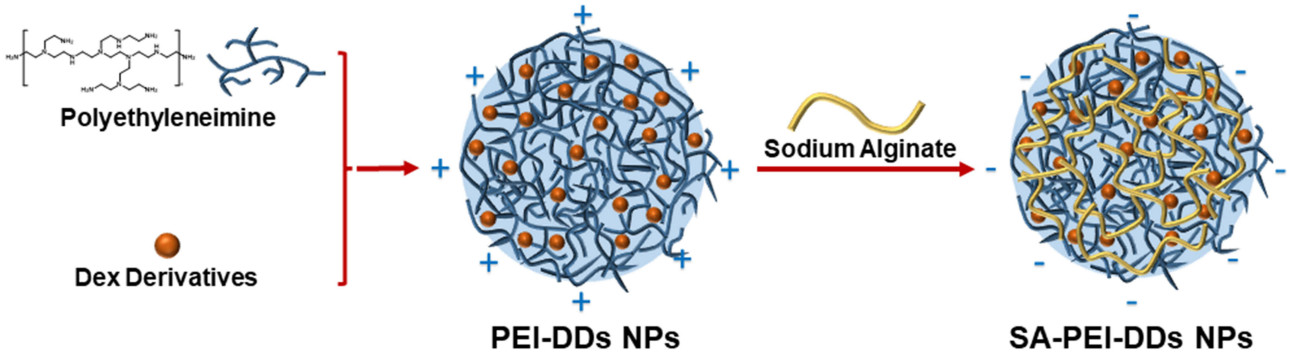

Scheme 1 Schematic illustration of the preparation of SA-PEI-DDs nanoparticles.

Experimental Methods

Materials

Dex, 2,4,6-Trinitrobenzenesulfonic acid (TNBS), and fluorescein isothiocyanate (FITC) were purchased from Sigma-Aldrich Co. (St Louis, MO, USA). Succinic anhydride, 4-dimethylaminopyridine, pyrophosphoryl chloride, triethylamine, O-Dianisidine dihydrochloride (ODD) and ethylenediaminetetraacetic acid (EDTA) were purchased from the Aladdin Chemistry Co. Ltd. (Shanghai, China). Dimethyl sulfoxide (DMSO), ethanol, ethyl acetate, pyridine, polyethyleneimine, seaweed sodium, calcium chloride, dimethyl sulfoxide, potassium dihydrogen phosphate and sodium hydroxide were Kermel Chemical Co. Ltd. (Tianjin, China). All other reagents were analytical grade and obtained from commercially available sources.

Animals

Male BALB/c mice (20 ± 2 g) were purchased from the Laboratory Animal Center of Xi'an Jiaotong University. Mice had ad libitum access to water and food under controlled temperature (20–25 °C) and relative humidity conditions (50–60%). They were quarantined for one week before treatment. The animal care and experimental protocols are in strict accordance with the Guidelines of the Laboratory Animal Center of Xi'an Jiaotong University and approved by the Institutional Animal Care and Use Committee of Xi'an Jiaotong University (No. XJTULAC 2019–068).

Synthesis of Dex Derivatives (DDs)

The DDs fabricated in this part were dexamethasone hemisuccinate (DSH) and dexamethasone phosphate (DSP), and the synthesis routes were shown in Figure 1 and described as follows: (1) fabrication of DSH: dexamethasone (1 g, 2.55 mmol) and an appropriate amount of 4-DMAP were mixed and dissolved in dry anhydrous acetone. Succinic anhydride (0.51 g, 5.10 mmol) was added to this mixture, followed by adding an appropriate amount of triethylamine dropwise, sealing, and stirring at room temperature for 1 h. Then, the impurities were removed from the product solution by suction filtration. The acetone was removed by rotary evaporation to obtain the oily and viscous products, which were then dissolved in absolute ethanol and mixed with distilled water (60 °C) to generate the precipitates. The residue was redissolved in anhydrous acetone, followed by heating reflux, and stood at 4 °C for 24 h to precipitate and crystallize, and then repeatedly washed with ethanol (25%) and dried to obtain white crystalline products. (2) Fabrication of DSP: dexamethasone (1 g, 2.55 mmol) was added to anhydrous tetrahydrofuran, followed by slowly adding pyrophosphoryl chloride dropwise with lowering the temperature. The reaction continued for 1 h. Then the reaction solution was diluted by adding deionized water and raising the temperature to 60 °C. A certain amount of Na_2CO_3 was added to the reaction solution and continued reacting for 0.5 h. the crude products were first filtered, then precipitated by dropwise adding hydrochloric acid. After being washed repeatedly with the hydrochloric acid solution, the final white solid powder was obtained and dried. All the final products were characterized by the nuclear magnetic resonance hydrogen spectrum (^{1}H-NMR Bruker, Germany) and the high-resolution mass spectrometry (MS, Thermo Scientific Q Exactive, USA).

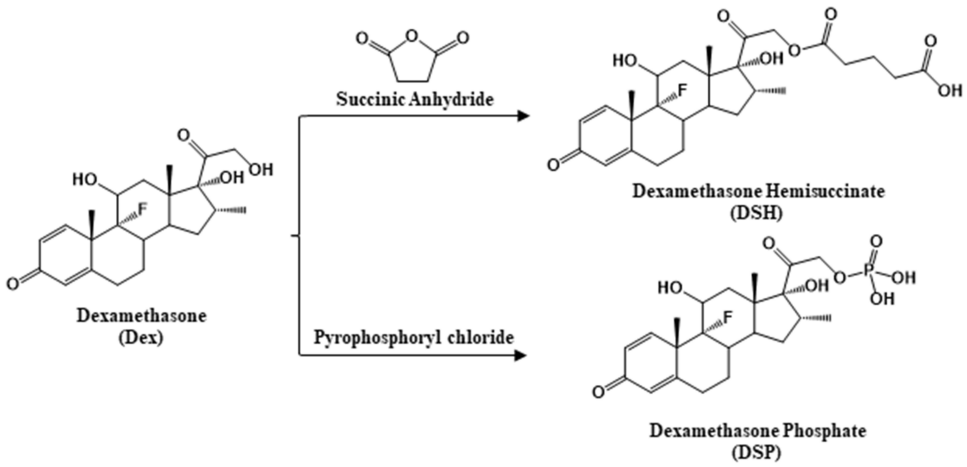

Figure 1 Synthetic schematic diagram of DSH and DSP.

Establishment of in vitro Analytical Methods for DDs

DSH or DSP (10 mg) were added to volumetric flasks (10 mL), respectively, followed by methanol to dissolve and dilute to the final concentration of 1 mg/mL. (1) Determining detection wavelength: diluting the above DDs solution to 0.01 mg/mL. The maximum absorption wavelength of different derivatives was determined by scanning with an ultraviolet-visible spectrophotometer (UV-vis, UV2550, Shimadzu, Japan) in the wavelength range of 200–800 nm, which was then used as the detection wavelength of the methodological research. (2) Development of the standard curve: preparing the methanol solutions of the above glucocorticoid derivative (0.1 mg/mL), pipetting 0.5, 1, 1.5, 2, 2.5 mL of these solutions into a 10 mL volumetric flask, and then diluted with methanol to 10 mL to obtain the concentrations of these DDs solutions at 0.005, 0.01, 0.015, 0.02, 0.025 mg/mL, respectively. Setting the blank methanol solution as the reference solution, the absorbance of different concentrations of DDs solutions was measured at the detection wavelength by UV-spectrophotometer. The standard curve was obtained by plotting the absorbance of each analyte versus DDs concentration. (3) Precision and recoveries tests: For the evaluation of precision, these different DDs samples of three different concentrations (0.005, 0.015, and 0.025 mg/mL) were processed and detected five times within a day (intra-day) and within five days (inter-day) by a UV-spectrophotometer for calculating RSD, respectively. To evaluate the adding sample recovery, different DDs with concentrations of 0.005, 0.015, and 0.025 mg/mL were prepared. DDs equivalent to 80%, 100%, and 120% of the initial content was added to these samples.[34] Then, the content of DDs in each sample was detected to calculate the recovery rate.

Preparation and Characterization of SA-PEI-DDs NPs

DDs were precisely weighed (10 mg) respectively, mixed with PEI (10 mg), and then dissolved in dimethyl sulfoxide (DMSO). The mixed solution was added to a dialysis bag (MWCO 3.5kDa) and immersed in deionized water to make the negatively charged DDs and positively charged PEI self-assemble to form NPs through the electrostatic interaction. The dialysate was replaced every 6 h, and the solution in the dialysis bag was taken out after 24 h, then freeze-dried to obtain PEI-DDs NPs. Furthermore, A certain amount of PEI-DDs NPs was added to the deionized water to form the suspension. Then, a certain volume of SA solution with appropriate concentration was added dropwise to the suspension, followed by stirring for 30 min at room temperature. The SA-PEI-DDs NPs were obtained after repeated washing, centrifugation, and lyophilization. The particle size, zeta potential, and polydispersity index (PDI) of SA-PEI-DDs NPs were detected by the dynamic light scattering (DLS, Malvern Zetasizer Naso ZS, Malvern, UK), and the morphology of SA-PEI-DDs NPs was characterized by transmission electron microscopy (TEM, H600, Hitachi, Japan). Moreover, during the fabrication process, the concentration of DDs, pH value, molecular weight of PEI, concentration of SA, and the feeding ratio of SA to PEI significantly influenced the formation of NPs. Therefore, a series of single-factor experiments were performed to explore the above factors' influence on forming SA-PEI-DDs NPs. Furthermore, the drug-loading coefficient (DL%) and entrapment efficiency (EE%) of DDs were calculated by the following equations, respectively:

$$DL\% = W_t/W_s\ 100\%$$

$$EE\% = W_t/W_0\ 100\%$$

Where W_t represented the weights of DDs in the final nanoparticles; W_s represented the weights of all components in the final nanoparticles. W_0 represented the weights of the feeding DDs.

Stability and in vitro Release Behavior of SA-PEI-DDs NPs

The in vitro stability of these SA-PEI-DDs NPs was detected by the DLS. Briefly, 5 mL SA-PEI-DDs NPs solutions were immersed in different medium solutions that simulated different environments of the gastrointestinal tract, namely artificial gastric juice (pH 1.2), artificial small intestinal juice (pH 6.8), and artificial colon juice (pH 7.4), respectively, and incubated for 0, 0.5, 2, 4, 8 and 12 hrs. At predetermined time intervals, solution (1 mL) was withdrawn and monitored with DLS (Malvern Zetasizer Naso ZS, Malvern, UK) to determine the particle size changes of SA-PEI-DDs NPs in different media.

For the in vitro release behavior study, two in vitro release experiments were set to explore and compare the differences in the release behavior of SA-PEI-DDs NPs after oral or enema administration, respectively. For the release experiments that mimic the release behavior of nanoparticles after oral administration, 5 mL SA-PEI-DDs NPs solution was successively added to the artificial gastric juice (pH 1.2) for 2 h, the artificial small intestinal juice (pH 6.8) for 4 h and the artificial colon juice (pH 7.4) for 6 h. For the experiments that mimic the release behavior of NPs after enema administration, 5mL SA-PEI-DDs NPs solution was only added to the artificial colon juice (pH 7.4) for 12h. In the two experiments, aliquots (1 mL) were withdrawn and replenished with an equal volume of fresh medium at predetermined time intervals. The samples were determined by the in vitro analytical methods for DDs in Preparation and Characterization of SA-PEI-DDs NPs to calculate the cumulative release rate of different DDs in NPs. All samples in release experiments were tested in triplicate in the above released experiments. The results at each time point were the relative value and the ratio of the tested value to the initial value.

Adhesion of SA-PEI-DDs NPs to the Isolated Colonic Mucosa

In this part, the adhesion of NPs to the isolated mouse colonic mucosa (normal mucosa and colonic inflammation mucosa) was investigated by examining the changes in the number of NPs in the solution after the incubation of isolated mouse colon tissue with different SA-PEI-DDs NPs solutions. The particle size and count rate (Kilo-count per second, Kcps) was selected as the investigation index detected by DLS (Malvern Zetasizer Naso ZS, Malvern, UK). The suspensions of PEI-DDs NPs and SA-PEI-DDs NPs based on different DDs were prepared, and their Kcps values were first determined. Then, the mice experimental colitis model was induced by the 2,4,6-trinitrobenzenesulfonic acid (TNBS). The specific method was as follows: mice were anesthetized with ether before induction of colitis after 12 h of fasting. 50% (v/v) ethanol (0.1 mL) which contained TNBS (2.5%, v/v) was instilled into the colon 3.5–4.0 cm from the anus by a gavage needle. Mice were kept in a head-down position for 30s to prevent the leakage of the intracolonic instillation.[35] After 12 h, the experimental colitis model mice were sacrificed to collect their colons. Colons were repeatedly washed with normal saline and then cut into small pieces with a length of 3 cm and longitudinal dissection. These issues were put into the PEI-DDs NPs and SA-PEI-DDs NPs suspensions of different DDs (0.5 mL) and incubated at 37 °C in the dark for 2 h. Then, the incubation solutions were taken out to measure the Kcps values, which were compared with the Kcps values determined by the NPs before incubation to calculate the percentage decrease in Kcps value to evaluate the adhesion of PEI-DDs NPs and SA-PEI-DDs NPs to the different isolated colonic mucosa. In this experiment, normal saline was also used instead of TNBS for modeling to establish a healthy mice control group. The treatment method was the same as that of the TNBS-induced experimental colitis model group.

In vivo Test of the Adhesion of SA-PEI-DDs NPs to the Colonic Mucosa

This part used fluorescein isothiocyanate (FITC) instead of DDs to co-construct SA-PEI-FITC NPs with PEI and SA. The specific preparation method was the same as that in Animals. Then, the experimental colitis model mice were induced by the TNBS, and the method was the same as in Stability and in vitro Release Behavior of SA-PEI-DDs NPs. The

experimental colitis model mice were fasted for 12 h and kept drinking water normally before the experiment. Then, FITC solution, PEI-FITC NPs solution, and SA-PEI-FITC NPs solution (1 mL) were administered by enema, respectively. The mice were sacrificed after 2 h, and the colons were taken out, longitudinally dissected, washed repeatedly with normal saline, and then spread on a glass slide. The confocal laser scanning microscope (CLSM, Leica TCS SP8, Germany) was used to observe the fluorescence intensity in the colon tissue of the mice. In this experiment, normal saline was also used instead of TNBS for modeling to establish a healthy mice control group. The treatment method was the same as that of the TNBS-induced experimental colitis model group.

Ameliorative Effects of SA-PEI-DDs NPs on Experimental Colitis

The mice experimental colitis model was induced according to the procedure in Stability and in vitro Release Behavior of SA-PEI-DDs NPs. Mice in the control group received normal saline instead of TNBS solution. The mice were randomly divided into 6 groups: (1) control-no colitis induced (enema normal saline, n=10), (2) TNBS (n=10), (3) TNBS+Dex (enema normal saline, 70 μg/kg Dex, n=10), (4) TNBS+SA-PEI-DSH NPs (enema 70 μg/kg according to the concentration of DSH, n=10). (5) TNBS+SA-PEI-DSP NPs (enema 70 μg/kg according to the concentration of DSP, n=10). The treatment was given after the induction of colitis for 12 h. During the experiment, the body weight changes of the mice in each group were recorded. The mice's feces were collected daily, followed by observing the characteristics of feces and measuring the fecal occult blood. The above data were aggregated to measure the disease activity index (DAI). The experiment was continued for 5 days, and the number of final surviving mice was recorded at the end of the experiment to calculate the final survival rate. Then, all of the mice in the respective groups were sacrificed, and the distal colons were taken out to measure their length. Next, the colon tissue was cut longitudinally along the mesentery and rinsed with ice-cold saline to remove the feces. The treated colon tissue was divided into two parts: one was employed in the myeloperoxidase (MPO) activity test after the homogenization, and the other was used for histopathological observation after being fixed with paraformaldehyde, embedded in paraffin sectioned, and stained with hematoxylin and eosin (H&E).

For DAI measurement, a small amount of feces was smeared on the white plate. 2–3 drops of o-tolidine (10 g/L) dissolved in glacial acetic acid were dripped into the feces and blended evenly, followed by adding 2–3 drops of 3% H_2O_2 solution, timing as well as observing the results immediately. The evaluation criteria of fecal occult blood level are shown in Table 1. Moreover, the fecal occult blood index was combined with body weight change and fecal character to calculate the DAI score, whose scoring standard was manifested in Table 2. The weighted tissue samples were homogenized in ten volumes of ice-cold phosphate buffer (50 mM K_2HPO_4, pH 6.0) for the MPO activity detection, containing 0.5% (w/v) HTAB. The homogenate was centrifuged at 10,000 rpm for 10min at 4 °C to discard the supernatant. The precipitate was homogenized with an equivalent volume of 50 mM K_2HPO_4 containing 0.5% (w/v) HTAB and 10 mM EDTA. The hydrogen-peroxide-dependent oxidation of o-dianisidine dihydrochloride (ODD) was measured to assess the MPO activity. One enzyme unit was defined as the amount of enzyme-producing one absorbance change per minute at 460 nm (37 °C). The enzyme activity was calculated as U/g tissue. The concentrations of pro-inflammatory cytokines, TNF-α, IL-6, and IL-1β, were determined from the homogenates using enzyme-linked immunoassay (ELISA) kits (Beyotime Biotechnology Co. Ltd, Shanghai, China), following the manufacturer's instructions.

Table 1 The Assay Criteria of o-Benzidine to Determine the Fecal Occult Blood of Mice

Results	Phenomenon
Normal	No color occurred after adding reagents for 2 min
Occult blood	Green or light green appears after adding reagent for 2min
Occult blood+	Blue-green or dark green appears after adding reagent for 10s
Occult blood++	Blue or blue-green appears after adding reagent for 5–20s
Occult blood+++	Dark blue appears immediately after the reagent is added

Table 2 Disease Activity Index Scoring Criteria

Weight Loss	Character of Faeces	Occult Blood	Score
<0%	Normal	Normal	0
1–5%	Loose	Occult blood+	1
5–10%		Occult blood++	2
10–15%	Diarrhea	Occult blood+++	3
>15%		Visible blood in the stool	4

Statistical Analysis

In this study, all quantitative results were presented as mean ± SD. Results in stability and in vitro release behavior study, mucoadhesion study, and anti-experimental ulcerative colitis study were analyzed by one-way ANOVA and LSD test using SPSS Statistical Software (v.22; IBM, Chicago, IL, USA). $p < 0.05$ was considered to be statistically significant.

Results and Discussion

Characterization and the Establishment of in vitro Analytical Methods for DDs

GCs have powerful anti-inflammatory effects and can treat UC by exerting the following functions: (1) Reducing capillary permeability to relieve inflammatory edema and exudation. (2) Binding to activated glucocorticoid receptors reduces the generation of pro-inflammatory factors by inhibiting NF-κB activity. (3) Reducing the generation of leukotrienes and prostaglandins by increasing lipocortin synthesis and inhibiting cyclooxygenase expression. (4) Regulating inflammation-related genes to inhibit cytokine storm production. (5) Reduces the inflammatory response by decreasing the accumulation of neutrophils and macrophages in the inflammatory area. However, long-term oral administration of GCs produces many systemic toxic and side effects. Therefore, it is necessary to concentrate GCs on the inflammatory colon site to improve the local treatment effect and reduce the systemic response. Some researchers have used low-dose GCs enema administration in the treatment process and achieved good results. This study synthesized two Dex derivatives, DSH (with carboxylate group) and DSP (with phosphate group), through esterification to construct a nano-drug delivery system with the adhesion effect of inflammatory mucosa to further improve the enrichment and retention time of dexamethasone (Dex) in the mucosa of colitis and improve the therapeutic effect.

The Dex was reacted with succinic anhydride and pyrophosphoryl chloride through an esterification reaction to construct DSH and DSP. The obtained products were characterized by ^{1}H-NMR and high-resolution MS. Figure 2A showed the ^{1}H-NMR spectrum of DSH: ^{1}H-NMR (600MHz, DMSO-d_6, δ: ppm): 0.886 (d, 3H, C_{16}-H), 1.030 (s, 3H, C_{18}-H), 1.614 (s, 3H, C_{19}-H), 2.744 (m, 4H, C_{22}-H, C_{23}-H), 6.103 (s, 1H, C_4-H), 6.034 (d, 1H, C_2-H), 7.427 (d, 1H, C_1-H). The MS results showed that the protonated molecular ion ($[M+H]^+$) peak was at 493.2. Figure 2B showed the ^{1}H-NMR spectrum of DSP: ^{1}H-NMR (600 MHz, DMSO-d_6, δ: ppm): 0.762 (m, 3H, C_{18}-H), 1.365 (d, 3H, C_{22}-H), 2.200 (m, 3H, C_{19}-H3), 2.502 (s, 1H, C_{16}-H), 5.108 (s, 1H, C_4-H), 5.407 (m, 1H, C_2-H), 5.562 (m, 1H, C_1- H). The MS results showed that the peak of the protonated molecular ion ($[M+H]^+$) was 463.2. These results all demonstrated the successful synthesis of these DDs.

In establishing in vitro analytical methods for DDs, their maximum absorption wavelengths detected by UV-vis spectra analysis were 241 nm (Figure S1). The linear relationships within the 0.005–0.025 mg/mL range were found between peak areas of each DAD concentration and theoretical concentrations (Figure S2). For precision detection, the intra- and inter-day RSD of the Dex derivative was less than 15% in three concentrations. For recovery detection, the adding sample recovery of different Dex derivative concentrations ranged from 99.64% to 100.71%, and no noticeable difference occurred among the three concentrations (Tables S1 and S2). These results indicated that the reproducibility and recovery were acceptable over the studied concentration range.

Preparation and Characterization of SA-PEI-DDs NPs

The self-assembled mucoadhesive NPs are formed by the spontaneous combination of hydrophilic or amphiphilic polymers under multiple noncovalent forces (electrostatic force, van der Waals force, hydrogen bond, hydrophobic force, π-π stacking, etc.), which enable the systems' stable structure and good thermodynamic stability.[36–38] The systems'

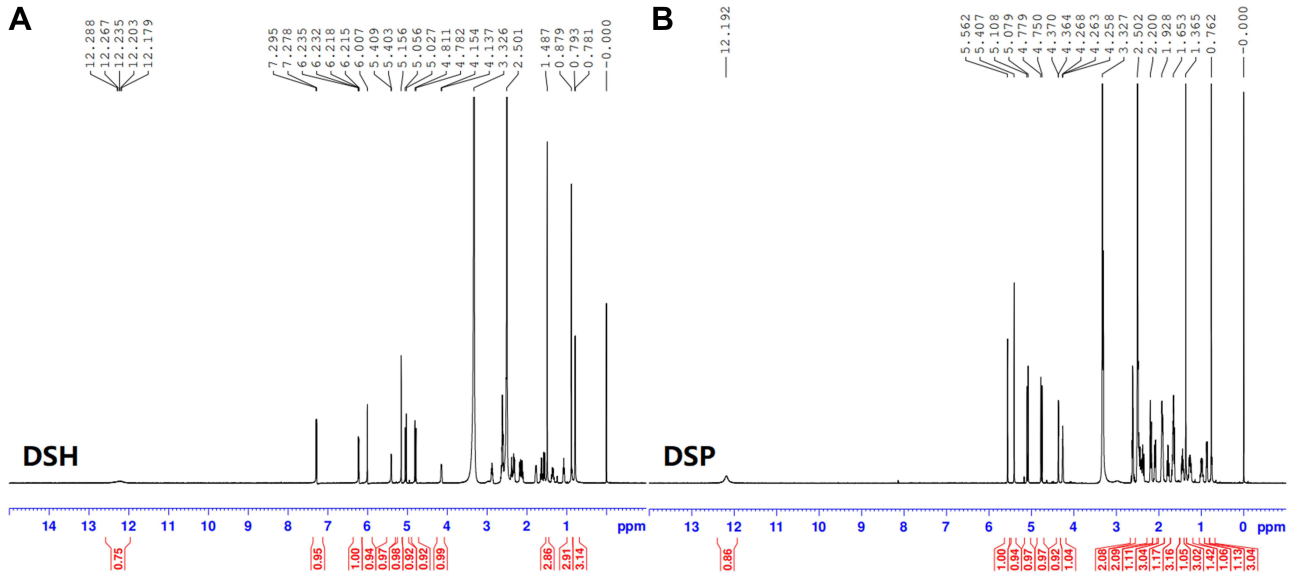

Figure 2 ^{1}H-NMR spectrum of DSH (**A**) and DSP (**B**).

preparation method is simple and can achieve high drug-loading efficiency. Therefore, this study first used the hydrophobic Dex to react with acidic anhydrides and acid chlorides to obtain the DDs with good water solubility and negative charges. Then, the DDs and the cationic polymer, PEI, were self-assembled to form the PEI-DDs NPs through electrostatic force. PEI-DDs NPs were finally encapsulated with the natural polyanionic polysaccharide, SA, to obtain SA-PEI-DDs NPs with surface charge inversion.

During the fabrication process, multiple factors significantly affected the final particle size, potential, and dispersibility of SA-PEI-DDs NPs. The influences of Dex derivatives' concentration, pH value, and PEI molecular weight on the PEI-DDs NPs are shown in Figure 3 and Tables S3–S5. From Figure 3A and B, and Table S3, the particle size, Zeta potential, and PDI all showed continuous decrease trends in different DDs groups as their concentration increased, mainly due to the significant increase of the negative charge in the solution with the increase of the DDs' concentration. In addition, the hydrophobic interactions and hydrogen bonding forces caused by the Dex structure itself and its hydroxyl groups respectively further aggravated the electrostatic interaction between the DDs and the positively charged PEI, thereby rapidly forming nanostructures and reducing the mutual aggregation of PEI, resulting in a decrease in particle size and Zeta potential. Figure 3C and D and Table S4 showed that the smallest particle sizes appeared at the neutral pH value (pH 7) but increased at acidic and alkaline pH values, indicating that both hydrogen ions (H^{+}) and hydroxyl ions (OH^{-}) could affect the electrostatic coupling between DDs and PEI increase particle size. Moreover, the growth of the negative charge in the solution also affected the Zeta potential and dispersibility of PEI-GC NPs. It was worth noting that the particle sizes of PEI-DSP NPs were significantly smaller than that of PEI-DSH NPs in the two situations, which might be because the DSP, as a kind of phosphate, is more negatively charged than DSH (the Dex carboxylate), leading to the stronger electrostatic adsorption between DSP and PEI, and forming the denser and smaller nanostructure. The effect of PEI molecular weight on the fabrication of PEI-GC NPs is shown in Table S5. Results showed that the particle size of NPs formed by low molecular weight PEI (Mn=1800) and DDs was significantly larger than that of high molecular weight PEI (Mn=25,000). It might be due to the fewer amino groups in the low molecular weight PEI that results in the weak electrostatic force between PEI and DDs. However, the high molecular weight PEI could interact with DDs through more amino groups in its structure and fabricate the structurally strong NPs.

SA is one of the main components for the construction of final NPs. Its concentration plays an essential role in the surface charge reversal of SA-PEI-DDs NPs and the realization of inflammatory mucosal adhesion. Besides, the feeding ratio (mass ratio) of SA to PEI also affects the morphology, potential, and dispersion of the final NPs. From Tables S6 and S7, the particle sizes of all SA-PEI-DDs NPs increased with SA concentration, and the same situation also occurred

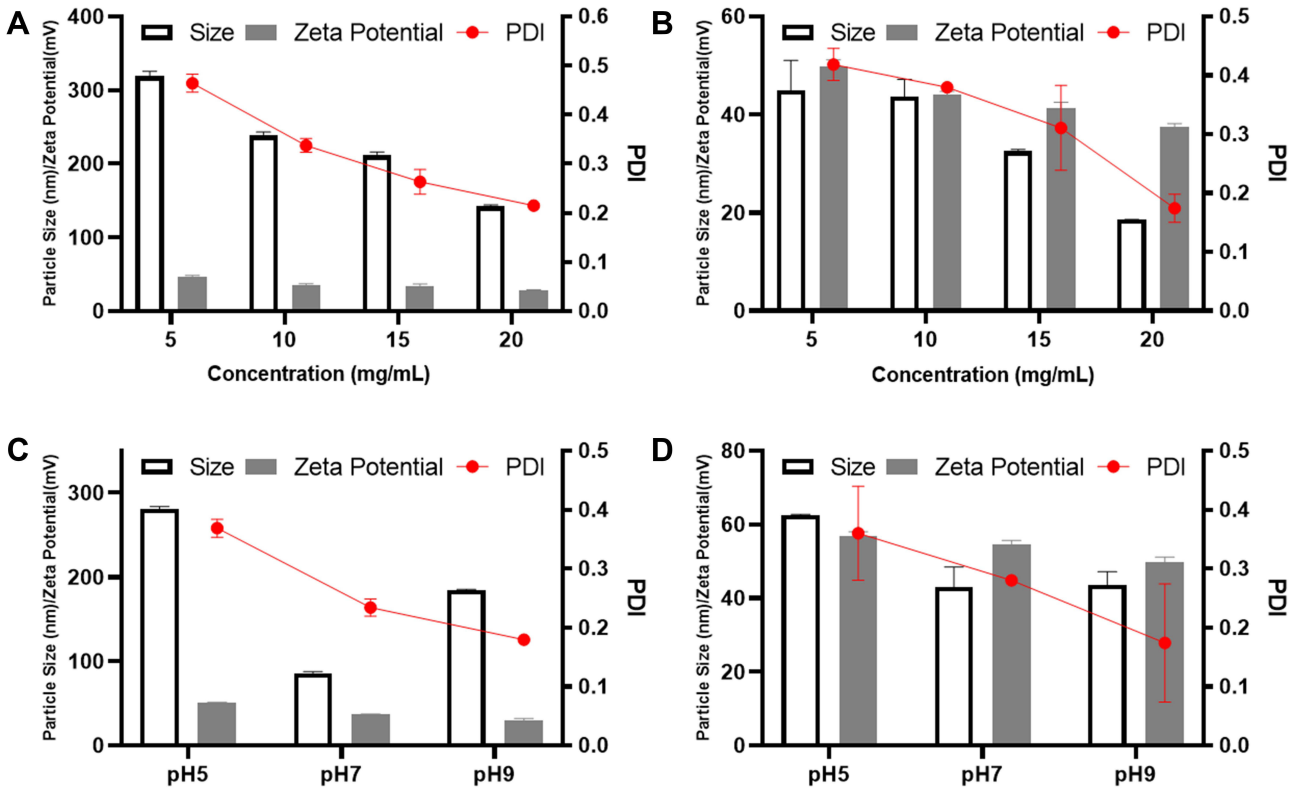

Figure 3 Effects of concentration and pH changes of Dex anion derivatives (DDs) on preparing PEI-DDs NPs. (**A** and **B**). Effects of concentration changes of DSH (**A**) and DSP (**B**) on the particle sizes, Zeta potential, and PDI of PEI-DSH and PEI-DSP NPs. (**C** and **D**). Effects of pH values on particle size, potential, and PDI of PEI-DSH NPs (**C**) and PEI-DSP NPs (**D**) (Mean ± SD, n = 3).

in the verification test of the feed ratio (mass ratio) of SA and PEI, indicating that as a high molecular anionic polysaccharide, the electrostatic adsorption of SA with cationic polymers increases with the increase of SA concentration and its concentration ratio in the total system. It was worth noting that the precipitation occurred when the SA concentration was 2 mg/mL and the feeding ratio of SA to PEI was 0.5:1, which might be because that excessive SA rapidly agglomerates with PEI through electrostatic adsorption to result in precipitation, and the NPs formed by DSH had a larger particle size and further increased to generate precipitation after mixing with SA. The above results show that SA could be adsorbed on the surface of PEI-DDs NPs by electrostatic force, which caused the increase in particle size and reversed the surface charge of the PEI-DDs NPs to form negatively charged SA-PEI-DDs NPs. Therefore, the optimal preparation formula of SA-PEI-DDs NPs was as follows: PEI molecular weight 25,000, pH 7, the concentrations of Dex derivative and SA were concentrated at 20 mg/mL, and 1 mg/mL, respectively, and the feed ratio of SA to PEI was 1:1. The characterization data of the final NPs prepared by the optimized process were shown in Table 3, and the TEM characterization results are shown in Figure 4. These results indicated that the particle size of final NPs increased significantly after SA coating. Since the electrostatic adsorption between DSP and PEI was stronger than that of DSH, the formed PEI-DSP and SA-PEI-DSP NPs were smaller than the latter. Besides, the final SA-PEI-DDs NPs were powerfully negatively charged and achieved high-efficiency loading on DDs (the drug-loading coefficients were more significant than 15%), thus promoting their adhesion to positively charged colonic inflammatory mucosa and improving the therapeutic effect by increasing the absorption of Dex at the colonic inflammatory site.

Stability and in vitro Release Behavior Study

The in vitro stability investigation of SA-PEI-DSH and SA-PEI-DSP NPs was shown in Figure 5A and B. The particle size changes of these SA-PEI-DDs NPs in different media solutions simulating the gastrointestinal tract environment showed similar laws, namely that the particle size of NPs increased the most in the artificial gastric juice, then slowed

Table 3 Characterization Data of SA-PEI-GC NPs (Mean ± SD, n = 3)

Parameters	SA-PEI-DSH-NPs	SA-PEI-DSP-NPs
Particle Size (nm)	196.33 ± 0.75	94.36 ± 2.28
Zeta Potential (mV)	−34.63 ± 0.77	−46.19 ± 0.25
PDI	0.25 ± 0.020	0.27 ± 0.010
Drug-loading coefficient (%)	27.40 ± 0.080	19.060 ± 0.26
Entrapment efficiency (%)	54.80 ± 0.16	76.24 ± 1.040

down in artificial intestinal juice and exhibited the smallest increase in the artificial colonic fluid. These results indicated that under strongly acidic conditions (pH 1.2), many protons generated electrostatic attraction with the negatively-charged SA on the surface of SA-PEI-DDs NPs. Moreover, protons also penetrated the NPs and caused electrostatic repulsion with PEI, which destroyed the multiple noncovalent forces (such as electrostatic force, hydrogen bond force, etc.) among DDs, PEI, and SA and resulted in the structural destruction of self-assembled NPs, finally leading to the significant increase of the particle sizes. However, the influence of protons on SA-PEI-DDs NPs gradually weakened with the rise of the pH value, resulting in slower growth in particle size. Under weak alkaline conditions (pH 7.4), the electrostatic repulsion between negatively charged hydroxyl ions and SA on the surface of NPs made them maintain structural integrity. Moreover, the hydroxyl ions with low concentration showed weak effects on the multiple noncovalent forces among the internal components of SA-PEI-DDs NPs, manifesting as a slight increase in particle sizes. It was worth noting that the particle size increase of SA-PEI-DSP NPs was smaller than that of SA-PEI-DSH NPs under acidic conditions, which was due to the DSPs carrying more negative charges, resulting in a more potent electrostatic force between it and the PEI, finally leading to the more stable NPs under acidic conditions.

The in vitro release results of different SA-PEI-DDs NPs are shown in Figure 5C and D. In the release experiment simulating oral administration conditions (Figure 5C), these SA-PEI-DDs NPs showed a burst release in the acidic environment of the simulated upper gastrointestinal tract, releasing large amounts of DDs. The cumulative release rate of SA-PEI-DSP NPs at each time point was lower than that of SA-PEI-DSH NPs, which might also be due to the stronger electrostatic force between DSP and PEI, making the NPs degrade more slowly

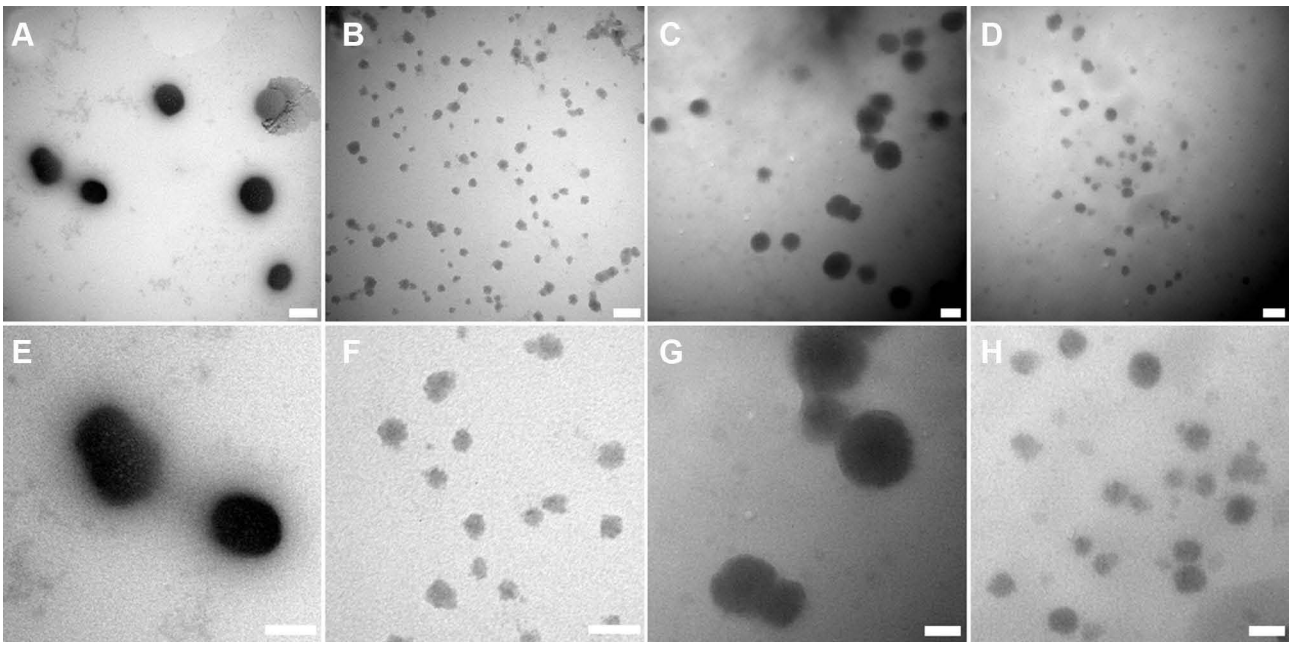

Figure 4 TEM images of PEI-DDs NPs. (**A** and **E**). PEI-DSH NPs. (**B** and **F**). PEI-DSP NPs. (**C** and **G**). SA-PEI-DSH NPs. (**D** and **H**). SA-PEI-DSP NPs. The sizes of TEM images: (**A** and **B**), scale bars: 100 nm; (**C** and **D**), scale bars: 200 nm; (**E** and **F**), scale bars: 50 nm; (**G** and **H**), scale bars: 100 nm.

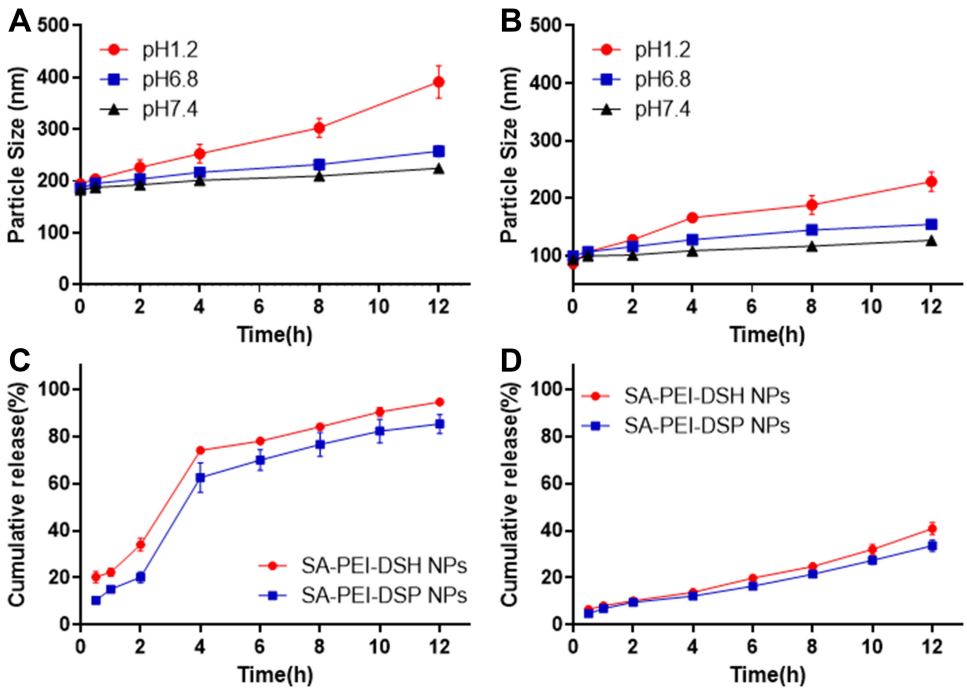

Figure 5 Stability and in vitro release behavior study. (**A** and **B**). Effect of the media solutions with different pH values on the particle size changes of different SA-PEI-DSH NPs (**A**) and SA-PEI-DSP NPs (**B**). (**C**). The in vitro release behavior of SA-PEI-DDs NPs in a release medium with different pH values. The experiment was successively conducted at pH 1.2 (from 0 to 2 h), pH 6.8 (from 3 to 6 h), and pH 7.4 (from 7 to 10 h). (**D**). The in vitro release behavior of SA-PEI-DDs NPs in a release medium of pH 7.4 for 12 h (mean ± SD, n = 3).

and resulting in minor DSP release. In the release experiment simulating enema administration (Figure 5D), the cumulative release rate of the two NPs media increased slowly, and the final cumulative release rate was about 40%. These results indicated that the solution pH significantly affected the stability and release behavior of SA-PEI-DDs NPs. At low pH, the protons could accelerate the release of DDs by affecting the composition and structure of NPs. However, in the high pH environment, the hydroxyl ions with the same surface charge as the NPs showed little effect on SA-PEI-DDs NPs, making them stable for a long time. Therefore, this type of NPs was more suitable for enema administration and remained stable in the alkaline colonic fluid environment before reaching the colonic inflammatory mucosa after administration, reducing the probability of early drug leakage.

The Mucoadhesion Study of SA-PEI-DDs NPs

This part used ex vivo and in vivo experiments to investigate the adhesion ability of SA-PEI-DDs NPs to colonic mucosa under physiological or pathological conditions. The adhesion of SA-PEI-DDs NPs to the isolated colonic mucosa was evaluated by the reduction of Kcps upon incubation with colon tissues from normal and colitis mice, respectively. Kcps is the intensity of the light scattering signal measured in count/s, which could be used for assessing the degree of adsorption of SA-PEI-DDs NPs in isolated colonic tissue.[39,40] Figure 6A showed the Kcps value variations of PEI-DDs NPs and SA-PEI-DDs NPs in the colonic mucosa of healthy mice. The PEI-DDs NPs treated groups showed a greater reduced Kcps compared with that of the SA-PEI-DDs NPs treated groups ($p < 0.05$), which was due to the electrostatic adsorption of the positively charged PEI-DDs NPs on the surface of the negatively charged normal colon tissue mucosa, resulting in more NPs adhering to the mucosa. Moreover, The Kcps value of the PEI-DSP NPs treated group decreased significantly than that of the PEI-DSH NPs treated group, which might be because the particle size of the PEI-DSP NPs was smaller than that of the PEI-DSH NPs, thus making more PEI-DSP NPs adhered to the colon tissue under the same conditions. The results from Figure 6B showed the opposite results from Figure 6A, namely that the SA-PEI-DDs NPs treated groups exerted more significant Kcps values reductions compared with that of the PEI-DDs NPs treated groups ($p < 0.05$), which

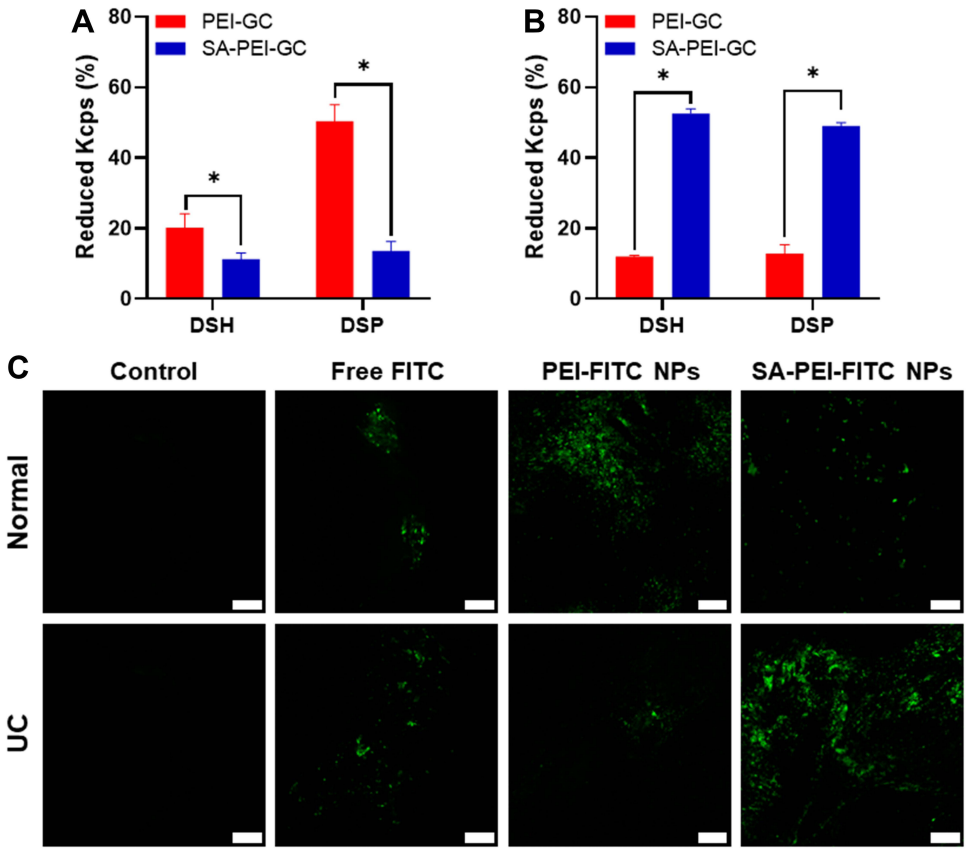

Figure 6 The ex vivo and in vivo mucoadhesion studies of SA-PEI-DDs NPs. (**A** and **B**). The adhesion of isolated colonic mucosa by using colon tissue from Healthy mice (**A**) and mice with UC (**B**). *$p < 0.05$: significantly different from the PEI-DDs NPs treated group, mean ± SD, n = 3. (**C**). The CLSM images of colon tissue after mice were given different FITC preparations by enema administration for 2 h (scale bars: 100 μm).

was mainly because the positively charged inflamed colon tissue mucosa could adsorb more negatively charged SA-PEI-DDs NPs to its surface through the electrostatic adsorption.

Furthermore, the in vivo adhesion of SA-PEI-DDs NPs to the colonic mucosa was investigated using the fluorescent molecules, FITC, instead of DDs to construct the SA-PEI-FITC NPs and detected by CLSM since FITC has a similar molecular weight (Mn:389) and charge to Dex (Mn: 392).[41,42] After enema administration of FITC solution or fluorescent NPs for 2 h, the amount of FITC-loaded NPs associated with the colon of mice was observed by CLSM. The intensity of green fluorescence in normal and inflamed colon tissues is shown in Figure 6C. Normal and UC mice receiving FITC solution show weak fluorescence in the colon. Normal mice treated with PEI-FITC-NPs solution showed higher green fluorescence intensity than those receiving SA-PEI-FITC-NPs. However, the UC mice that received SA-PEI -FITC-NPs exhibited the highest fluorescence intensity than other groups. The results confirm that the negatively charged SA-PEI-FITC-NPs could enhance the adhesion to inflamed mucosa with positive charges through the enema administration, thereby improving the targeting of nanoparticles to the site of colon inflammation and further increasing local drug concentration in inflamed tissues, which was consistent with the in vitro adhesion results.

Anti-Inflammatory Effects of NPs

The anti-experimental colitis experiment lasted for 5 days and all mice survived at the end of the experiment. The weight loss degree in mice is one of the critical indicators for assessing the severity of UC. From Figures 7A and S3A, compared with the normal saline-treated group, the body weights of the other groups of mice after TNBS modeling showed decreasing trends to varying degrees. However, the weight-loss trend of the mice in each treatment group was reversed after 2 days of treatment, indicating that these therapeutic formulations inhibited TNBS-induced colitis. It was worth noting that the final body weight

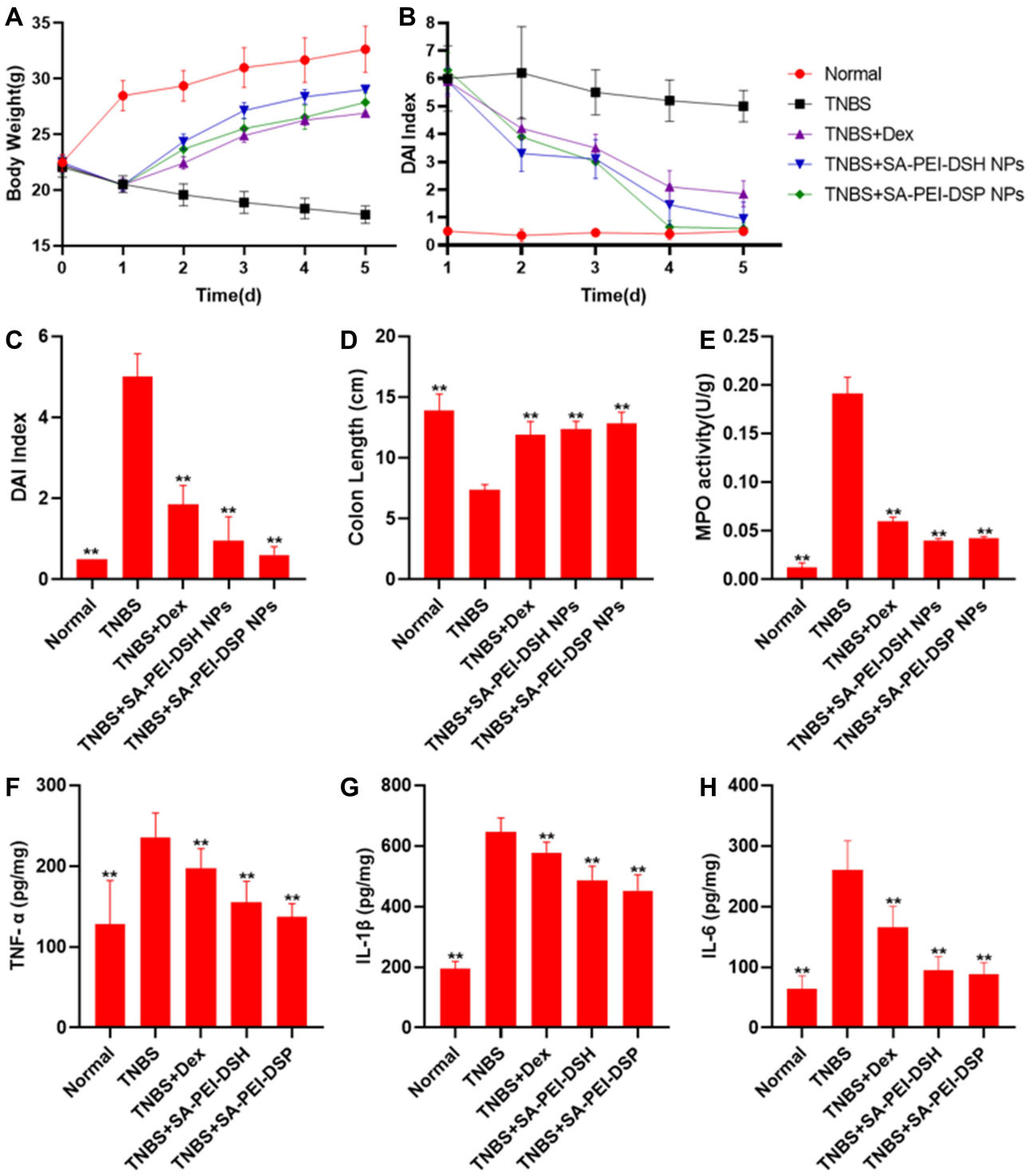

Figure 7 The anti-ulcerative colitis effects of SA-PEI-DDs NPs. (**A**). The influence of SA-PEI-DDs NPs on the body weight changes of mice. (**B**) and (**C**). The influence of SA-PEI-DDs NPs on the variation of DAI index of mice (**B**) and the ultimate DAI index (on the 5th day) of mice treated with different Dex preparations (**C**). (**D**). The colon length of mice in each group after the experiment. E. The influence of SA-PEI-DDs NPs on MPO activity in the colon tissue of mice. (**F**–**H**). Effects of SA-PEI-DDs NPs on the expression of TNF-α (**F**) and IL-1 β (**G**) and IL-6 (**H**) in mouse colon tissue. $^{**}p < 0.01$: significantly different from the TNPS-treated group, mean ± SD, n = 10.

recovery of mice treated with different SA-PEI-DDs was much higher than that of the free Dex-treated group, indicating the better effects of NPs than free Dex.

Once inducing the experimental colitis, the mice appeared with some conditions, including bloody stools, diarrhea, reduced activity, and weight loss after 24 h. DAI is the aggregated indicator after a quantitative analysis of these

conditions.[35,43,44] After being modeled by TNBS, the mice of the TNBS group and other therapy groups developed the conditions like bloody stools, diarrhea, decreased activity, and weight loss, and their DAI significantly increased. On 2nd day of treatment, The DAI index of other treatment groups except the TNBS group has shown a downward trend. After 5 days of treatment, the DAI index of all treatment groups was significantly decreased compared with the TNBS group ($p < 0.01$), and the DAIs of these SA-PEI-DDs groups decreased more than that of the free Dex group, whose final DAI values were almost the same as that of the normal group, indicating that SA-PEI-DDs achieved better anti-inflammatory effect than the free GCs (Figure 7B and D and S3B). The mice were sacrificed on the last day of therapy, and the colons were taken out to measure their length, as shown in Figure 7D. Compared with the normal group and each treatment group, the colon length of the TNBS group was significantly shortened. Besides, the colon lengths in the NPs treated groups were more prolonged than in the free Dex group.

MPO is a heme protease with the prosthetic group of heme, which belong to the heme peroxidase superfamily. MPO is present in the aniline blue granules of myeloid cells (eg, neutrophils and monocytes) and is the marker of myeloid cells.[45] Therefore, MPO activity is often used as one of the essential indicators to evaluate inflammation degree since MPO activity increases sharply and is released into the extracellular fluid under the inflammatory state.[46,47] As shown in Figure 7E, the MPO activity of mice in the TNBS group was significantly higher than that in the normal group and all treatment groups ($p < 0.01$), indicating the significant development of inflammation after the TNBS induction. However, after the treatment with different preparations, the MPO activity of each treatment group decreased, and their decrease degrees were more substantial than that in the free Dex group, indicating that the inflammation relief degree by NPs was better than that of the Dex. The UC severity is also related to the number of inflammatory cytokines. As shown in Figure 7F–H, the levels of the proinflammatory cytokine TNF-α, IL-1β, and IL-6, in the colon tissues of the three treatment groups were significantly decreased compared with the TNBS group. These indicators of the two NPs groups were lower than that of the free Dex group under the same dose conditions, indicating the excellent improvement of NPs on inflammation. It is noteworthy that in the above treatment indices, the parameters of the SA-PEI-DSP NPs treated group were always slightly better than those of the SA-PEI-DSH NPs treated group, which might be related to the tight binding of DSP with more negative charges to PEI, making more DSP be transported to the inflammation site after enema administration. In addition, the particle size of SA-PEI-DSP NPs was smaller than that of SA-PEI-DSH NPs, which can adhere more to the colitic mucosa under the same conditions, thereby targeting the inflammatory colon tissue through the eEPR effect to achieve the therapeutic effect.

The colon histopathological changes were observed by H&E staining further to evaluate the severity of UC in each group. As shown in Figure 8, the colonic mucosal epithelial barrier was complete and continuous in the normal group. The glands were regularly arranged, and there was no inflammatory cell infiltration in the lamina propria. On the contrary, the colonic mucosal barrier of the TNBS group was destroyed, together with edematous submucosa, structurally

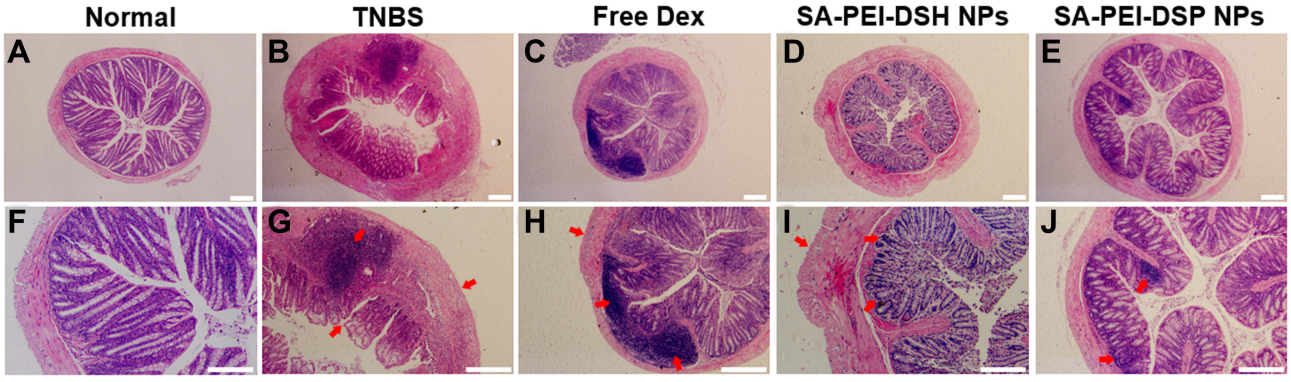

Figure 8 Histological sections of the colon stained with hematoxylin and eosin (HE). (**A**–**E**). Complete colon sections in different treatment groups, scale bars: 200 μm. (**F**–**J**). Local magnified view of colon sections in different treatment groups, corresponding to figure (**A**–**E**), respectively, scale bars: 100 μm. The area indicated by the arrow: TNBS group: the colon crypt structures are collapsed with significant inflammatory cell infiltration, and the intestinal wall is significantly thickened; Free Dex group: significant inflammatory cell infiltration appeared in colon tissues with the thickened intestinal wall; SA-PEI-DSH NPs group: the intestinal wall is thickened and partial colon tissues showed inflammatory cell infiltration; SA-PEI-DSP NPs group: local colon tissues showed inflammatory cell infiltration.

abnormal glands, and disappeared crypt structures, accompanied by a large number of inflammatory cell infiltration. Each treatment group's colonic mucosal epithelial structure was intact, with decreased inflammatory cell infiltration in lamina propria. The colonic histology and morphology of mice treated with SA-PEI-DDs NPs were almost the same as those in the normal group, indicating that the inflammation degree of mice in each group treated was significantly reduced after being treated with SA-PEI-DDs NPs.

Conclusion

To summarize, we have constructed a kind of mucoadhesive NPs. The core PEI-DDs NPs were built by the electrostatic adsorption of the DDs and the PEI. Then, the SA was electrostatically coated around the core NPs to construct the final SA-PEI-DDs NPs. The changes in material concentration and pH during the fabrication process significantly affected the morphology of final NPs. The SA-PEI-DDs NPs showed good stability and adhesion of colitis mucosa in the colon environment, which is conducive to the enrichment of Dex in the colitis sites and enhances the therapeutic effect of Dex. The in vivo anti-UC studies revealed that the SA-PEI-DDs NPs exhibited a better therapeutic effect than free Dex on the experimental colitis mice induced TNBS through enema administration. The above results indicated that mucoadhesive NPs could achieve highly effective colon targeting by enema administration, which also had great potential as a novel nano-enema for treating UC.

Acknowledgment

This work was supported financially by the National Natural Science Foundation of China (No. 81973253, 81803491, 81773663), the China Postdoctoral Science Foundation (No. 2021M702633), the Key R&D Program Project for Shaanxi Province (No. 2022SF-081, 2020SF-218), the Fundamental Research Funds for the Central Universities (No. xxj032021004) and the National Undergraduate Innovation and Entrepreneurship Training Program (No. S202110698182). The authors thank the Instrument Analysis Center of Xi'an Jiaotong University for the help and funding (Subsidy fund for the operation of large instruments and equipment, No. YB2022051) on the characterization.

Disclosure

The authors report no conflicts of interest in this work.

References

1. Ungaro R, Mehandru S, Allen PB, Peyrin-Biroulet L, Colombel JF. Ulcerative colitis. *Lancet*. 2017;389(10080):1756–1770. doi:10.1016/S0140-6736(16)32126-2
2. Gajendran M, Loganathan P, Jimenez G, et al. A comprehensive review and update on ulcerative colitis. *Dm Dis Month*. 2019;65:12.
3. Loren V, Cabre E, Ojanguren I, et al. Interleukin-10 enhances the intestinal epithelial barrier in the presence of corticosteroids through p38 MAPK activity in Caco-2 Monolayers: a possible mechanism for steroid responsiveness in ulcerative colitis. *PLoS One*. 2015;10:6. doi:10.1371/journal.pone.0130921
4. George LA, Cross RK. Treatment of ulcerative colitis with steroids (in whom, how long, what dose, what form). *Gastroenterol Clin North Am*. 2020;49(4):705–716. doi:10.1016/j.gtc.2020.08.001
5. Salice M, Rizzello F, Calabrese C, Calandrini L, Gionchetti P. A current overview of corticosteroid use in active ulcerative colitis. *Expert Rev Gastroenterol Hepatol*. 2019;13(6):557–561. doi:10.1080/17474124.2019.1604219
6. Van Molle W, Libert C. How glucocorticoids control their own strength and the balance between pro- and anti-inflammatory mediators. *Eur J Immunol*. 2005;35(12):3396–3399. doi:10.1002/eji.200535556
7. Uchida K, Araki T, Toiyama Y, et al. Preoperative steroid-related complications in Japanese pediatric patients with ulcerative colitis. *Dis Colon Rectum*. 2006;49(1):74–79. doi:10.1007/s10350-005-0213-7
8. Oray M, Abu Samra K, Ebrahimiadib N, Meese H, Foster CS. Long-term side effects of glucocorticoids. *Expert Opin Drug Saf*. 2016;15(4):457–465. doi:10.1517/14740338.2016.1140743
9. Kayal M, Shah S. Ulcerative colitis: current and emerging treatment strategies. *J Clin Med*. 2020;9:1.
10. Cohen RD, Dalal SR. Systematic review: rectal therapies for the treatment of distal forms of ulcerative colitis. *Inflamm Bowel Dis*. 2015;21(7):1719–1736. doi:10.1097/MIB.0000000000000379
11. Loew BJ, Siegel CA. Foam preparations for the treatment of ulcerative colitis. *Curr Drug Deliv*. 2012;9(4):338–344. doi:10.2174/156720112801323062
12. Hanauer S. Advantages in IBD: current developments in the treatment of inflammatory bowel diseases. *Gastroenterol Hepatol (N Y)*. 2010;6(5):309–316.
13. Ham M, Moss AC. Mesalamine in the treatment and maintenance of remission of ulcerative colitis. *Expert Rev Clin Pharmacol*. 2012;5(2):113–123. doi:10.1586/ecp.12.2
14. Yan ZX, Liu YM, Ma T, et al. Efficacy and safety of retention enema with traditional Chinese medicine for ulcerative colitis: a meta-analysis of randomized controlled trials. *Complement Ther Clin Pract*. 2021;42:1. doi:10.1016/j.ctcp.2020.101278

15. Tsuda M, Ohnishi S, Mizushima T, et al. Preventive effect of mesenchymal stem cell culture supernatant on luminal stricture after endoscopic submucosal dissection in the rectum of pigs. *Endoscopy*. 2018;50(10):1001–1016. doi:10.1055/a-0584-7262
16. Beuerlein KG, Bowers NL, Savas J, Strowd LC. Ulcerative lesions and diarrhea: answer. *Am J Dermatopathol*. 2022;44(5):387–388. doi:10.1097/DAD.0000000000002081
17. Binder HJ. Mechanisms of diarrhea in inflammatory bowel diseases. In: Fromm M, Schulzke JD, editors. *Molecular Structure and Function of the Tight Junction: From Basic Mechanisms to Clinical Manifestations*. Vol. 1165. John Wiley & Sons; 2009:285–293.
18. Salim SY, Soderholm JD. Importance of disrupted intestinal barrier in inflammatory bowel diseases. *Inflamm Bowel Dis*. 2011;17(1):362–381. doi:10.1002/ibd.21403
19. Zhou HY, Ikeuchi-Takahashi Y, Hattori Y, Onishi H. Nanogels of a succinylated glycol chitosan-succinyl prednisolone conjugate: release behavior, gastrointestinal distribution, and systemic absorption. *Int J Mol Sci*. 2020;21:7.
20. Xu S, Yang QQ, Wang RY, et al. Genetically engineered pH-responsive silk sericin nanospheres with efficient therapeutic effect on ulcerative colitis. *Acta Biomater*. 2022;144:81–95. doi:10.1016/j.actbio.2022.03.012
21. Jalanka J, Cheng J, Hiippala K, et al. Colonic mucosal microbiota and association of bacterial taxa with the expression of host antimicrobial peptides in pediatric ulcerative colitis. *Int J Mol Sci*. 2020;21:17. doi:10.3390/ijms21176044
22. Lj F, Gn F, Yy D, Lv P, Hy L. Bactericidal/permeability increasing protein gene polymorphism and inflammatory bowel diseases: meta-analysis of five case-control studies. *Int J Colorectal Dis*. 2017;32(3):433–435. doi:10.1007/s00384-016-2740-1
23. Zhang SF, Ermann J, Succi MD, et al. An inflammation-targeting hydrogel for local drug delivery in inflammatory bowel disease. *Sci Transl Med*. 2015;7:300. doi:10.1126/scitranslmed.aaa5657
24. Furuta R, Ando T, Watanabe O, et al. Rebamipide enema therapy as a treatment for patients with active distal ulcerative colitis. *J Gastroenterol Hepatol*. 2007;22(2):261–267. doi:10.1111/j.1440-1746.2006.04399.x
25. Uppalapati D, Sharma M, Aqrawe Z, et al. Micelle directed chemical polymerization of polypyrrole particles for the electrically triggered release of dexamethasone base and dexamethasone phosphate. *Int J Pharm*. 2018;543(1–2):38–45. doi:10.1016/j.ijpharm.2018.03.039
26. Fahira AI, Amalia R, Barliana MI, Gatera VA, Abdulah R. Polyethyleneimine (PEI) as a polymer-based co-delivery system for breast cancer therapy. *Breast Cancer Targets Ther*. 2022;14:71–83. doi:10.2147/BCTT.S350403
27. Wang X, Niu DC, Hu C, Li P. Polyethyleneimine-based nanocarriers for gene delivery. *Curr Pharm Des*. 2015;21(42):6140–6156. doi:10.2174/1381612821666151027152907
28. Wegmann F, Gartlan KH, Harandi AM, et al. Polyethyleneimine is a potent mucosal adjuvant for viral glycoprotein antigens. *Nat Biotechnol*. 2012;30(9):883–U116. doi:10.1038/nbt.2344
29. Kochkodan OD, Kochkodan VM, Sharma VK. Removal of Cu(II) in water by polymer enhanced ultrafiltration: influence of polymer nature and pH. *J Environ Sci Health a Tox*. 2018;53(1):33–38.
30. Helander IM, Latva-Kala K, Lounatmaa K. Permeabilizing action of polyethyleneimine on Salmonella typhimurium involves disruption of the outer membrane and interactions with lipopolysaccharide. *Microbiol UK*. 1998;144:385–390. doi:10.1099/00221287-144-2-385
31. Dong WF, Liu D, Zhang TT, You Q, Huang FJ, Wu J. Oral delivery of staphylococcal nuclease ameliorates DSS induced ulcerative colitis in mice via degrading intestinal neutrophil extracellular traps. *Ecotoxicol Environ Saf*. 2021;215:1. doi:10.1016/j.ecoenv.2021.112161
32. Oshi MA, Lee J, Kim J, et al. pH-responsive alginate-based microparticles for colon-targeted delivery of pure cyclosporine a crystals to treat ulcerative colitis. *Pharmaceutics*. 2021;13:9. doi:10.3390/pharmaceutics13091412
33. Sonmez S, Coyle C, Sifrim D, Woodland P. Duration of adhesion of swallowed alginates to distal oesophageal mucosa: implications for topical therapy of oesophageal diseases. *Aliment Pharmacol Ther*. 2020;52(3):442–448. doi:10.1111/apt.15884
34. Nam YS, Kwon IK, Lee Y, Lee KB. Quantitative monitoring of corticosteroids in cosmetic products manufactured in Korea using LC-MS/MS. *Forensic Sci Int*. 2012;220(1–3):E23–E28. doi:10.1016/j.forsciint.2011.12.011
35. Dong K, Zhang HF, Yan Y, et al. Improvement of side-effects and treatment on the experimental colitis in mice of a resin microcapsule-loading hydrocortisone sodium succinate. *Drug Dev Ind Pharm*. 2017;43(3):448–457. doi:10.1080/03639045.2016.1258410
36. Sun W, Mao SR, Mei D, Kissel T. Self-assembled polyelectrolyte nanocomplexes between chitosan derivatives and enoxaparin. *Eur J Pharm Biopharm*. 2008;69(2):417–425. doi:10.1016/j.ejpb.2008.01.016
37. Mao SR, Bakowsky U, Jintapattanakit A, Kissel T. Self-assembled polyelectrolyte nanocomplexes between chitosan derivatives and insulin. *J Pharm Sci*. 2006;95(5):1035–1048. doi:10.1002/jps.20520
38. Germershaus O, Mao SR, Sitterberg J, Bakowsky U, Kissel T. Gene delivery using chitosan, trimethyl chitosan or polyethylenglycol-graft-trimethyl chitosan block copolymers: establishment of structure-activity relationships in vitro. *J Control Release*. 2008;125(2):145–154. doi:10.1016/j.jconrel.2007.10.013
39. Yan Y, Sun Y, Wang PC, et al. Mucoadhesive nanoparticles-based oral drug delivery systems enhance ameliorative effects of low molecular weight heparin on experimental colitis. *Carbohydr Polym*. 2020;246:1. doi:10.1016/j.carbpol.2020.116660
40. Sun W, Mao SR, Wang YJ, et al. Bioadhesion and oral absorption of enoxaparin nanocomplexes. *Int J Pharm*. 2010;386(1–2):275–281. doi:10.1016/j.ijpharm.2009.11.025
41. Duff AF, Bielke LR, Relling AE. Technical note: fluorescein as an indicator of enteric mucosal barrier function in preruminant lambs. *J Anim Sci*. 2020;98:7. doi:10.1093/jas/skaa198
42. Joshi A, Keerthiprasad R, Jayant RD, Srivastava R. Nano-in-micro alginate based hybrid particles. *Carbohydr Polym*. 2010;81(4):790–798. doi:10.1016/j.carbpol.2010.03.050
43. Dong K, Zeng AG, Wang ML, et al. In vitro and in vivo study of a colon-targeting resin microcapsule loading a novel prodrug, 3,4,5-tributyryl shikimic acid. *Rsc Adv*. 2016;6(20):16882–16890. doi:10.1039/C5RA16971B
44. Yan Y, Ren FL, Wang PC, Sun Y, Xing JF. Synthesis and evaluation of a prodrug of 5-aminosalicylic acid for the treatment of ulcerative colitis. *Iran J Basic Med Sci*. 2019;22(12):1452–1461. doi:10.22038/IJBMS.2019.13991
45. Pinkus GS, Pinkus JL. Myeloperoxidase - a specific marker for myeloid cells in paraffin sections. *Modern Pathol*. 1991;4(6):733–741.
46. McCabe AJ, Dowhy M, Holm BA, Glick PL. Myeloperoxidase activity as a lung injury marker in the lamb model of congenital diaphragmatic hernia. *J Pediatr Surg*. 2001;36(2):334–336. doi:10.1053/jpsu.2001.20709
47. Tsai MS, Shaw HM, Li YJ, Lin MT, Lee WT, Chan KS. Myeloperoxidase in chronic kidney disease: role of visceral fat. *Nephrology*. 2014;19(3):136–142. doi:10.1111/nep.12187